XVI International Conference on Computational Plasticity. Fundamentals and Applications
COMPLAS 2021
E. Oñate, D. Peric, M. Chiumenti and Eduardo de Souza Neto (Eds)

NON-LOCAL NUMERICAL TREATMENT OF NON-LINEAR BEHAVIOR BY MEANS OF HELMHOLTZ EQUATION, WITH VARIABLE COEFFICIENTS. APPLICATION TO REINFORCED CONCRETE STRUCTURES

ROMAIN GONTERO[1], ALAIN MILLARD[2], THIERRY VIDAL[1], ALAIN SELLIER[1] AND LUCA SORELLI[3]

[1] LMDC, INSA/UPS Génie Civil
135 Avenue de Rangueil, 31077 Toulouse cedex 04 France
e-mail: gontero@insa-toulouse.fr, thierry.vidal@univ-tlse3.fr, alain.sellier@univ-tlse3.fr
web page: http://www-lmdc.insa-toulouse.fr/

[2] CEA DEN/DANS/DM2S/SEMT/LM2S
bâtiment 607 - CEN Saclay 91191 Gif sur Yvette cedex, France
e-mail: alain.millard@cea.fr - web page: https://www.cea.fr/

[3] UNIVERSITE LAVAL
2325 Rue de l'Université, Québec, QC G1V 0A6, Canada
e-mail: luca.sorelli@gci.ulaval.ca - web page: https://www.ulaval.ca/

Key words: Plasticity, Modeling, Reinforced Concrete, Sliding, Non-Local

Abstract. Numerous research works has been done with the aim of modeling the cracking of reinforced concrete (RC) structures. Among the recent methods proposed in the literature, the combination of reinforcement-concrete equilibrium with the linear behavior of their interface leads to a Helmholtz equation which takes account of the slip between the homogenized reinforcements and the concrete in presence of localized cracks. In the case of large cracks openings, it is necessary to consider the non-linear behaviors of materials and their interfaces, such as the plasticity of reinforcements. These phenomena induce variations of the coefficients in the Helmholtz equation, which leads to two levels of iterative procedures: one at a global level considering equilibrium of homogenized RC, and another one at a non-local level taking account of equilibrium between reinforcement and concrete. The implementation of a convergence criterion is then needed at each level. The goal of this paper is to describe the developments implemented in the Finite Element code Cast3m to perform non-local Helmholtz type calculations with non-constant coefficients. This method, using an acceleration method, is illustrated by the cases of reinforced concrete tie and beam, with homogenized reinforcements.

1 INTRODUCTION

Reinforced concrete structures are subject to cracking, which is in most case a necessary phenomena to maximize the reinforcements efficiency. However, the crack opening is a limit state that must be controlled because cracks are a preferential path for chemical aggression. Modeling the concrete cracking in presence of reinforcements is a challenging goal mostly because of the interactions between reinforcements and matrix during cracking. It is well known that during the cracking process, a sliding occurs between the reinforcement and the matrix, leading to a relaxation of the reinforcement, and affecting cracks number and their opening. Currently, the methods used to take into account this sliding, consist of meshing explicitly the reinforcements and their interfaces with the matrix, which is not suitable for large reinforced concrete structures [4],[5],[2],[8],[9]. To avoid meshing the reinforcements, it is possible to use an homogenized model, where only concrete elements are meshed, and reinforcements are given by their surface ratio and orientations vectors. The mechanical global equilibrium is then verified by taking into account stress in both matrix and reinforcement considering that the strain is the same for the two materials, and so prevent to consider sliding. However, a model taking into account the sliding in the case of homogenized reinforced concrete has been recently proposed [12]. This method has proven its efficiency in the case of linear behavior of reinforcement. The main objective of this paper is to describe the method used to consider non linear behavior of the reinforcement constitutive law.

2 Basics of the homogenized model

The model development proposed in this paper is based on a homogenized anisotropic model of reinforced concrete developed by Sellier et al. [10]. This model includes modeling of anisotropic rotating cracks in the concrete matrix, thanks to tensile plasticity. The present part gives the essentials explanations about the existing model.

2.1 Constitutive equations

The homogenized stress in the reinforced matrix σ_{ij} is obtained by summing the contribution of both the matrix and the reinforcement (1).

$$\sigma_{ij} = (1 - \sum_{n=1}^{N_r} \rho_n)\sigma_{ij}^{m} + \sum_{n=1}^{N_r} \rho_n \sigma_{ij}^{rn} \tag{1}$$

In (1), ρ_n is the surfacic ratio of steel in a given direction, N_r is the total types of reinforcements, σ_{ij}^{m} the stress in the matrix and σ_{ij}^{rn} the stress in the reinforcement number n.

2.1.1 Stresses in the matrix

The stress in the matrix is assessed thanks to a model described in [11] based on the damage theory [7], which is extended to macro-cracks. Evolution of the damages are computed thanks to the plastic principal's strains, which control the anisotropic cracks in tension. This allows to support three rotating orthotropic cracks directions following the principals tensile strains directions. In a principal direction of stresses I, the damaged stress in the matrix is expressed by (2).

$$\sigma_I^m = (1 - D^c)(C_I^c \widetilde{\sigma}_I^{m-} + (1 - D_I^t)\widetilde{\sigma}_I^{m+}) \tag{2}$$

In (2), the stress $\widetilde{\sigma}_I^{m-}$ is the compressive stress while $\widetilde{\sigma}_I^{m+}$ is the tensile stress. D^c is the isotropic shear damage based on the plastic shear deformations. For shear stresses, the plastic deformations are computed thanks to a Drucker-Prager criterion. C^c is a crack reclosure criterion which varies between 0 when the crack is open, to 1 when the crack is completely closed. D_I^t stands for the tensile damages occurring in a principal direction I. The tensile damage depends on the principals plastic tensile strains ϵ^{pl} which occur when the Rankine tensile criterion is reached. They are linked by the relation (3), where w_I^k is a parameter depending on the fracture energy G_f which leads to the relation (4) where l_I is the finite element length in the direction I and R_t the tensile strength of the matrix. These relations are related to the Hillerborg method [6] and allows that any size of finite element will dissipate the same fracture energy. It is important to note that in the model, the matrix strain is linked to the crack opening w_I by the relation $w_I = \epsilon_I^{pl} l_I$.

$$D_I^t = 1 - \left(\frac{w_I^k}{w_I^k + max(w_I^{pl})} \right)^2 \tag{3}$$

$$G_f = \int_0^{+\infty} \sigma_I^m d\epsilon_I^{pl} \simeq R_t w_I^k \tag{4}$$

As shown in (2), an isotropic damage in shear and compression D^c can occur. This damage is computed thanks to the material plastic dilatancy $Tr(\bar{\bar{\epsilon}}^{pl,c})$ (5), where Tr is the trace of the second order tensor. The compressive plastic strains $\epsilon^{pl,c}$ are computed thanks to a Drucker-Prager criterion, with a non associated plastic flow allowing the model to take into account the effective dilatancy of the concrete. In (5), $\epsilon^{k,s}$ is a characteristic strain which controls the evolution of the damage rate versus dilatancy. Figure 1 gives a concrete single finite element response for the corresponding imposed displacement cycle.

$$D^c = \frac{Tr(\bar{\bar{\epsilon}}^{pl,c})}{Tr(\bar{\bar{\epsilon}}^{pl,c}) + \epsilon^{k,s}} \tag{5}$$

2.1.2 Stresses in reinforcements

The stress in the reinforcement n is obtained thanks to an orientation tensor P_{ij}^{rn}. This orientation tensor can be written as (6).

$$P_{ij}^{rn} = e_i^{\bar{r}n} \otimes e_j^{\bar{r}n} \tag{6}$$

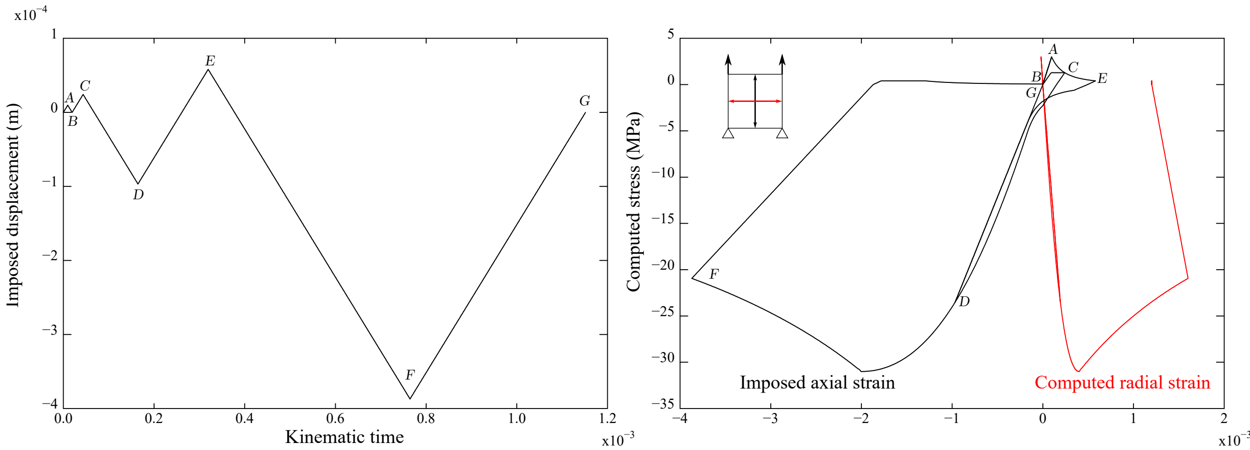

Figure 1: Response of the model for the concrete matrix alone in uniaxial cyclic test, with $E^m = 31$ GPa, $R_c^m = 31.1$ MPa, $R_t^m = 3$ MPa, $G_f = 100\,\mathrm{J/m^2}$, for a single finite element.

In (6), the $\overrightarrow{e^{rn}}$ vector is a unit vector obtained directly from the coordinates of the orientation vector of the reinforcement n. As the reinforcements in the matrix are uni-axial, the undamaged stress in the reinforcement $\widetilde{\sigma}^r_{ij}$ is obtained using (7).

$$\widetilde{\sigma}^r_{ij} = E^r(\epsilon^r - \epsilon^{r,pl})P^{rn}_{ij} \tag{7}$$

In (7), E^r is the Young modulus of the reinforcement, ϵ^r is its axial strain and $\epsilon^{r,pl}$ its plastic strain. The behavior law used for the reinforcement is composed of three phases. Elastic phase develops until the elasticity limit f^r_y. Then, a linear kinematic hardening phase occurs, it is characterized by its hardening modulus H^r. To prevent the stress in reinforcement to increase to inconsistent values, a damage has been added to its behavior law, leading to a horizontal asymptote. The damage is applied when the undamaged stress $\widetilde{\sigma}^r$ reaches the ultimate limit stress f^r_u, so the stress in the reinforcement cannot exceed the value of f^r_u. The damage affecting the tensile response of a reinforcement is given by relation (8).

$$D^r = \begin{cases} 0 & \text{if} \quad \widetilde{\sigma}^r < f^r_u \\ 1 - \dfrac{f^r_u}{\widetilde{\sigma}^r} & \text{if} \quad f^r_u \leq \widetilde{\sigma}^r \end{cases} \tag{8}$$

As a damage cannot decrease, a consistence condition $\dfrac{\partial D^r}{\partial t} \geq 0$ is added. The reinforcement tensile behavior law is shown in figure 2.

2.2 Interface between matrix and reinforcement

An imperfect bond is used between the matrix and its steel reinforcements, so that, the homogenized reinforcements can slip from the matrix. This slip is accounted for by means of Helmholtz equation given in (9). This last is obtained from reinforcement equilibrium

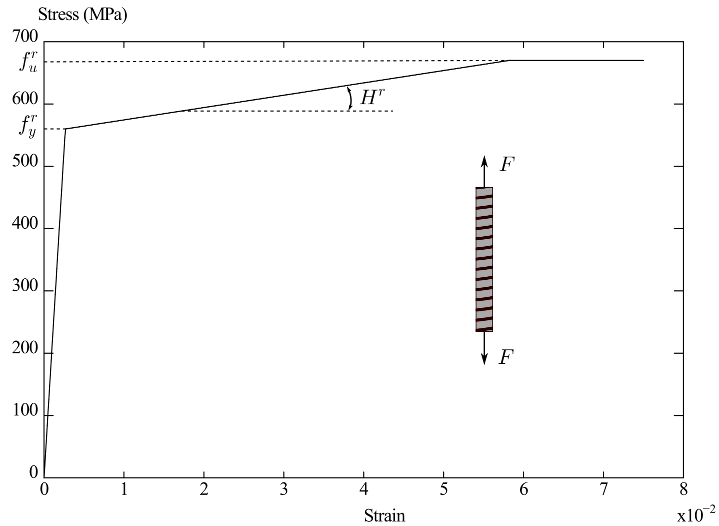

Figure 2: Tensile behavior of homogenized finite element 10 cm length with 100% of reinforcement, $E^r = 210000$ MPa, $f_y^r = 560$ MPa, $H^r = 2000$ MPa, $f_u^r = 670$ MPa.

equation, combined with a relation between the interface shear stress and sliding, the behavior law of the reinforcement and a link between sliding and strains of both materials. The original Helmholtz equation was presented in [12], where the elastic strain in the reinforcement was the state variable to be solved. In the present work, this formulation is reformulated in term of total stress in the reinforcement, taking into account its eventual damage D^r. This reformulation is needed to minimize the number of terms including derivatives.

$$\sigma^r - \frac{(1-D^r)E^r\Phi^r}{4H^i}\frac{\partial^2\sigma^r}{\partial x^2} = (1-D^r)E^r\left(\epsilon^m - \epsilon^{r,pl}\right) \tag{9}$$

In (9), σ^r is the total stress in the reinforcement along its abscissa x, D^r is the damage in the reinforcement, Φ^r is the reinforcement diameter, H^i is the shear stiffness of the interface, ϵ^m the matrix total strain in the reinforcement direction and $\epsilon^{r,pl}$ the plastic axial strain of the reinforcement. This relation assumes a constant tangent stiffness between the matrix and the reinforcement for a maximum sliding of 0.5 mm which correspond to a crack opening up to 1 mm. This Helmholtz equation acts as a diffusion equation, where the source to be diffused is the difference between the strain of the matrix and the anelastic strain of the reinforcement weighted by the damaged Young modulus of the reinforcement. It can be written in the form given in (10), where l_c^r is homogeneous to a diffusion length, and S is the source term of the diffusion.

$$\sigma^r - \frac{l_c^{r2}}{2}\frac{\partial^2\sigma^r}{\partial x^2} = S \tag{10}$$

It can be seen that the reinforcement damage D^r allows to consider the fact that when a damage occurs in the reinforcement, the phenomena become localized by reducing the

Helmholtz diffusive coefficient. Due to the damage in the diffusion term, and the plastic strain in the source term, the differential equation becomes non linear, and the objective of the present work is to treat numerically this non linearity.

3 Finite element implementation

The governing equations to be solved consist of the global equilibrium of the reinforced concrete and the stress in the reinforcement n given by the second order formulation (11). These equations are solved considering their variational formulations discretized on the finite element mesh. This implementation is described in [12], where only the elastic phase of the reinforcement was considered. To take into account the non linearity of the reinforcement behavior, it is necessary to implement an iterative procedure which consist of stabilizing the stress in the reinforcement compared to the concrete strain. This procedure needs to be implemented between two global equilibrium iterations.

$$\begin{cases} \displaystyle\sum_{j=1}^{3} \frac{\partial \sigma_{ij}}{\partial x_j} + f_i = 0 \qquad \text{for } i \in [1,\,2,\,3] \\ \sigma_n^r - \dfrac{l_{cn}^{r\,2}}{2} \dfrac{\partial^2 \sigma_n^r}{\partial x_n^2} = S_n \qquad \text{for } n \in [1, ..., N^r] \end{cases} \tag{11}$$

The boundary conditions at the edges of the reinforcements are assuming that there is no sliding between the reinforcement and the matrix. It can be written $\frac{\partial \sigma^r}{\partial x} = 0$ which leads to $\frac{\partial \epsilon^r}{\partial x} = 0$ until the edges of the reinforcement doesn't plasticized. First, the matrix strain is proposed by the global finite element solver, it allows to construct the source term. Then, the Helmholtz equation is solved globally thanks to the method described in [12], and so leads to the stress in the reinforcement. If this stress value exceeds the elasticity limit or the ultimate stress of the reinforcement, the source needs to be actualized, and the Helmholtz equation has to be solved again. This sub-iteration procedure uses an implicit solver which consist of minimizing the residue of equation (10). Each values of the residue at the nodes of the mesh are considered as components of a residue vector. As the residue in the reinforcement is a vector, it is necessary to compute a scalar which is in correlation with this vector. The residue R^H to be minimized for all the N^r reinforcements is given by equation (12).

$$R^H = \max_{n=1,N^r} \left[\frac{\sqrt{\left(\bar{R}_n^r\right)^T \bar{R}_n^r}}{f_u^r} \right] \tag{12}$$

Where the residue vector is given by relation (13). As the residue uses the maximum value of all the N^r reinforcements, the solver iterates until all reinforcements are at equilibrium.

$$\bar{R}_n^r = \bar{\sigma}_n^r - \frac{l_{cn}^{r\,2}}{2} \frac{\partial^2 \bar{\sigma}_n^r}{\partial x_n^2} - \bar{S}_n \tag{13}$$

As the difference between the residues of two successive sub steps present a geometric convergence rate, it is possible to use an acceleration method based on the one proposed by Chow and Kay [3], inspired by Aitken's work [1].

$$\bar{\sigma}_{i+2}^{acc} = \bar{\sigma}_{i+1} + \lambda(\bar{\sigma}_{i+1} - \bar{\sigma}_i) \tag{14}$$

Where λ is a scalar relaxation factor, determined from three successive estimations of the vector $\bar{\sigma}$.

$$\lambda = \frac{(\bar{\sigma}_{i-1} - \bar{\sigma}_i)^T (\bar{\sigma}_i - \bar{\sigma}_{i+1})}{(\bar{\sigma}_{i-1} - \bar{\sigma}_i)^T (\bar{\sigma}_{i-1} - 2\bar{\sigma}_i + \bar{\sigma}_{i+1})} \tag{15}$$

4 Application

To illustrate the model abilities, this section contains two applications of the reinforcement sliding, the first one is a theoretical case, consisting of a tensile test on a reinforced concrete tie with a single crack. The second application is a real reinforced concrete beam submitted to a bending test with experimental data.

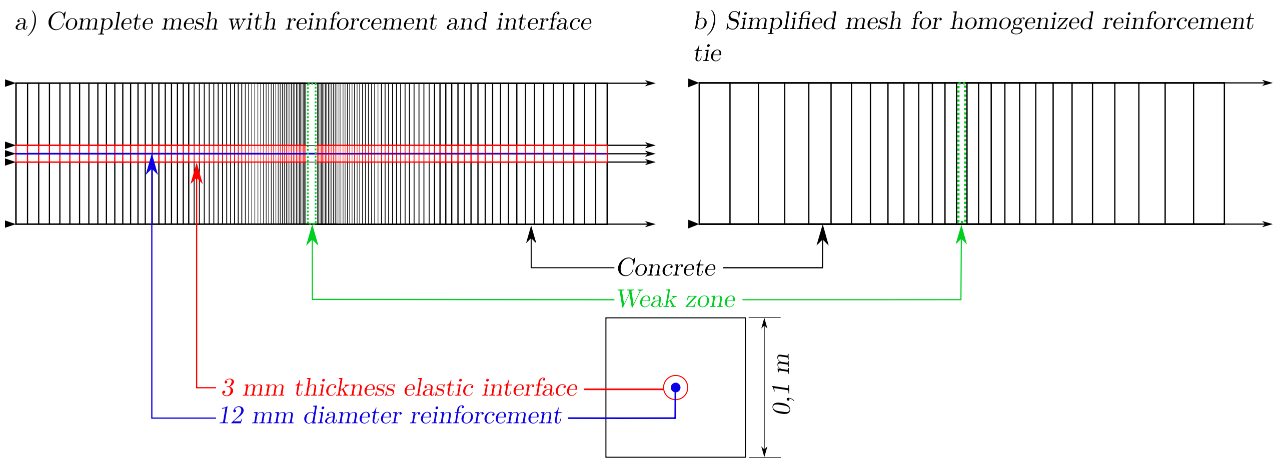

Figure 3: Mesh and boundary conditions for the two ties

4.1 Theoretical case

The purpose of this section is to study the numerical response of the model through the case of a concrete tie containing a single longitudinal reinforcement placed in the center of the cross-section. The homogenized tie results are compared to a reference case were both the reinforcement and the elastic interface are meshed. For the homogenized model, the reinforcement is only defined by its surfacic ratio all over the transverse section, and by its orientation vector. For both cases, the middle of the ties contains an element with a concrete tensile strength of 3 MPa, whereas all other elements are characterized by a concrete tensile

Parameter	Symbol	Value	Unit
	Concrete parameters		
Compressive strength	R_c	35	MPa
Tensile strength in the weak zone	R_t	3	MPa
Young's modulus	E^m	31000	MPa
Poisson's ratio	ν	0.2	-
Tensile fracture energy	G_f^m	100	J/m^2
	Reinforcement parameters		
Elastic limit	f_y^r	560	MPa
Young's modulus	E^r	210000	MPa
Hardening modulus	H^r	2000	MPa
Maximum stress	f_u^r	667	MPa
	Homogenized tie interface parameter		
Elastic shear stiffness	H^i	40000	MPa/m
	Reference tie interface parameters		
Elastic modulus	E^i	960	MPa
Poisson's ratio	ν^i	0	-

Table 1: Reinforced concrete ties parameters

strength of 30 MPa, in order to localize the crack only in the weak element (Figure 3). For the reference case, the reinforcement is meshed with unidimensional bars elements for which the behavior law has been plotted. Figure 3 gives both mesh and boundary conditions used. Only the tensile behavior is studied in this case. It can be seen that, in the reference case, the mesh next to the weak zone is highly refined compared to the homogenized case. This allows to get a better precision in the reference results.

Homogenized tie parameters - The material parameters and their values used to perform the test are given in Table 1. The concrete used can be classified as an ordinary concrete. The characteristics of the reinforcement are as well standards for civil engineering. The corresponding reinforcement ratio used is $\rho^r = 1.1\%$ of the tie transverse section.

Reference tie parameters - The elastic modulus E^i of the meshed interface is linked to the homogenized interface stiffness by the relation (16) obtained by the virtual work method, where ν^i is the meshed interface Poisson's ratio. This relation is determined such that the elastic energy is equivalent in both the homogenized tie and the reference case. All other concrete and reinforcement parameters are the same as in the homogenized case.

$$E^i = 2H^i\Phi^r(1+\nu^i) \tag{16}$$

Results - Figure 4 gives computed force versus displacement for the reference case and two of the homogenized case: one is done with a sub-iteration convergence tolerance of $R^H = 10^{-6}$ and the other one is done with only one sub-iteration. It can be seen the strong impact of the sub-iteration convergence tolerance to fit the reference evolution. It is important to note that, for small loading steps, both a) and b) curves would be the same. The implemented method allows therefore to use large loading steps which will activate the sub-iterations. This provides a security in the case of needed large loading steps. These results show that the reinforcement phenomenon linked to its plasticity is taking into account in the homogenized model. Even if the results are close, there is still a little shift in the plastic phase of reinforcement behavior. This can be explained by the fact that in the reference case, the solved variables consist of the nodes displacements, whereas the reinforcement stress is solved in the homogenized case. This implies a constant strain in finite elements of the reference case and a linear variation of the strain in the homogenized case, so it could be noted that the homogenized case is more smooth than the reference one.

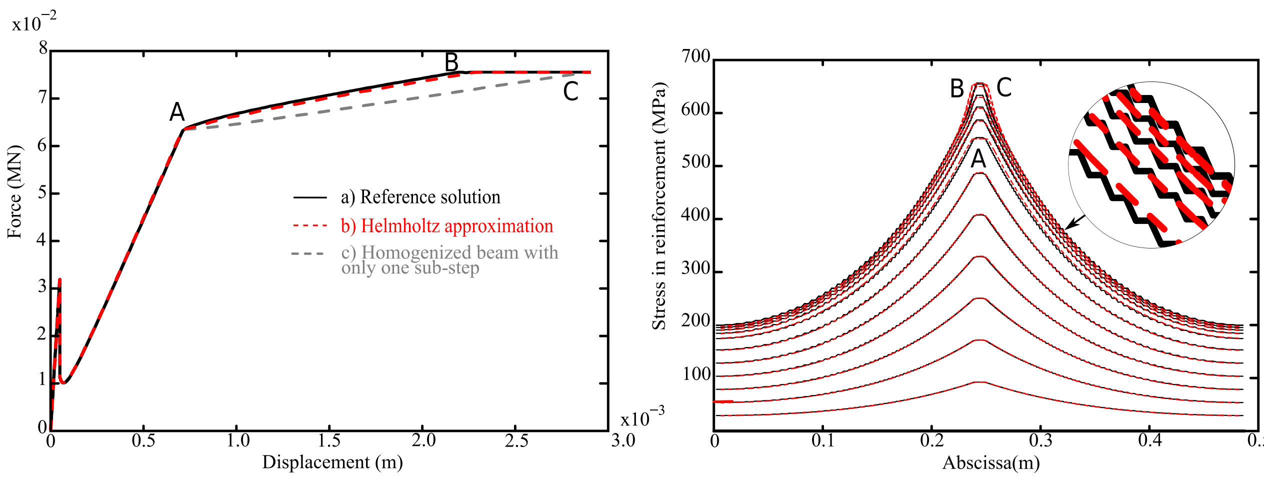

Figure 4: Comparison of the force-displacement curves for the two homogenized ties and the reference case.

4.2 Application to a real structure

After the theoretical validation, it is necessary to compare the model with a real structure behavior. The chosen case is a beam submitted to a four point bending test. The reinforced concrete parameters are given in Table 2. To show the sliding impact, results are compared with a case where the sliding is not considered between matrix and reinforcement by applying the same strain in both materials. Figure 5 compares the model results obtained with and without sliding of the reinforcements. Considering the force-deflection curves, it appears that both models are close of the experimental response. The sliding model is however more efficient in predicting the cracking process, as the non-sliding model make it imprecise. Looking at the cracking pattern during loading, reinforcement sliding allows a better localisation of each crack. Assuming an equal strain in matrix and reinforcement leads to higher stress in

Parameter	Symbol	Value	Unit
	Concrete parameters		
Compressive strength	R_c	37.4	MPa
Tensile strength	R_t	2.8	MPa
Young's modulus	E^m	32700	MPa
	Reinforcement parameters		
Elastic limit	f_y^r	520	MPa
Young's modulus	E^r	195000	MPa
Hardening modulus	H^r	3245	MPa
	Interface parameter		
Elastic shear stiffness	H^i	40000	MPa/m

Table 2: Reinforced concrete beam parameters

the matrix next to the cracks which causes diffused damage while sliding lets the matrix stress in the vicinity of the crack slowly increases as observed in figure 4. Crack pattern evolution has been reported during the test, and it is noticable that sliding model matches well with the real cracking pattern for each load. Figure 5 shows that sliding changes spacing between cracks as expected, as well as the cracks openings and the number of cracks at a given load.

5 Conclusion

A model allowing to take into account non linear behaviors of reinforcements and interfaces in the case of non meshed reinforcements has been presented. The model is based on solving a Helmholtz equation in parallel of the global equilibrium of the reinforced concrete. The non linearity induced by reinforcement plasticity and damage induces the need of an iterative procedure which has been implemented. A theoretical tie test has shown the ability of the model to find the reference case results during phases of elasticity, plasticity and damage of the reinforcement. In the case of the real structure, it was observed that the model is efficient in predicting both the global force-deflection response, but also the cracking pattern evolution thanks to reinforcement sliding. This model has proved that it is effective to predict the behavior of the reinforcement linked to concrete until the reinforcement maximal stress. Its use should not be limited to civil engineering purposes since it could be applied to several physics fields, which require diffusive variable in parallel of the global equilibrium.

Aknowledgements: The members of the C.E.A Jean-Charles Le Pallec, Ludovic Jason and Caroline Guerin are thanked for supporting this work.

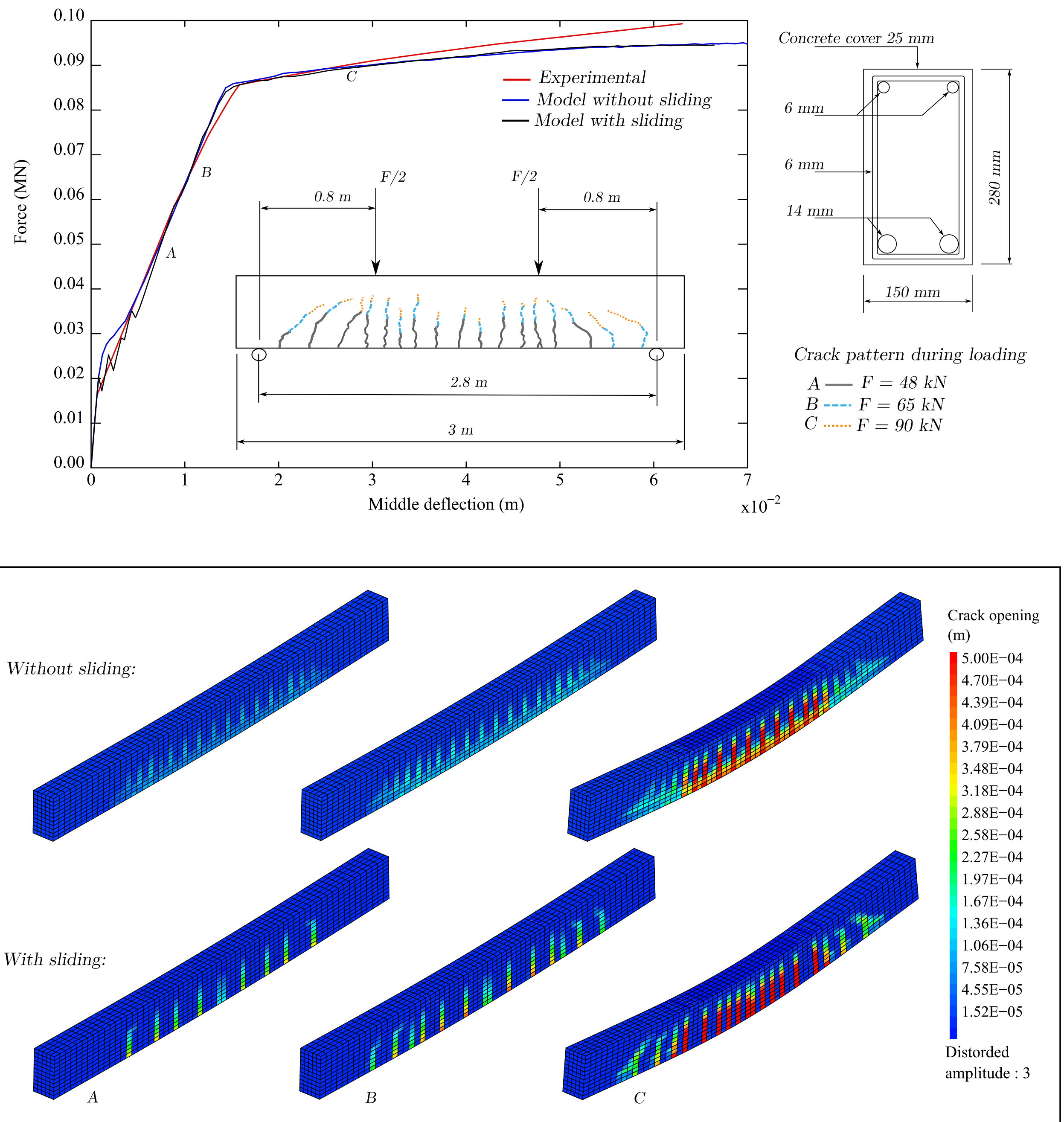

Figure 5: Geometric characteristics and results of the beam test : model and experimental force deflection curves, computed crack opening field for the beam with and without reinforcement sliding

REFERENCES

[1] A. C. Aitken. On the iterative solution of a system of linear equations. *Proc. Roy. Sot. Edinburgh*, pages 52–60, 1950.

[2] A. Casanova, L. Jason, and L. Davenne. Bond slip model for the simulation of reinforced concrete structures. *Engineering Structures*, 39:66–78, 2012.

[3] Y. K. Chow and S. Kay. On the Aitken acceleration method for nonlinear problems. 19(l):757–761, 1984.

[4] N. Dominguez, D. Brancherie, L. Davenne, and A. Ibrahimbegović. Prediction of crack pattern distribution in reinforced concrete by coupling a strong discontinuity model of concrete cracking and a bond-slip of reinforcement model. *Engineering Computations*, 22:558–582, 2005.

[5] R. Hameed, A. Turatsinze, F. Duprat, and A. Sellier. Bond stress-slip behaviour of steel reinforcing bar embedded in hybrid fiber-reinforced concrete. *KSCE Journal of Civil Engineering*, 17(7):1700–1707, oct 2013.

[6] A. Hillerborg, M. Modeer, and P. E. Peterssonn. Analysis of crack formation and crack growth in concrete by means of fracture mechanics and finite elements. *Cement and Concrete Research*, 6:773–782, 1976.

[7] J. Lemaitre and J. L. Chaboche. *Mécanique des matériaux solides*. Dunod, Paris, 1985.

[8] C. Mang, L. Jason, and L. Davenne. A new bond slip model for reinforced concrete structures : Validation by modelling a reinforced concrete tie. *Engineering Computations*, 32(7):1934–1958, 2015.

[9] C. Mang, L. Jason, and L. Davenne. Crack opening estimate in reinforced concrete walls using a steel–concrete bond model. *Archives of Civil and Mechanical Engineering*, 16(3):422–436, 2016.

[10] A. Sellier. Model FLUENDO3D Version 23-C for CASTEM 2017 Anisotropic Damage and Visco-Elasto-Plasticity Applied to Reinforced Multiphasic Materials, Technical Report. Technical report, LMDC, 2018.

[11] A. Sellier, G. Casaux-Ginestet, L. Buffo-Lacarrière, and X. Bourbon. Orthotropic Damage Coupled with Localised Crack Reclosure Processing. Part I: Constitutive Laws. *Engineering Fracture Mechanics*, 97l(January):148–167, oct 2013.

[12] A. Sellier and A. Millard. A homogenized formulation to account for sliding of non-meshed reinforcements during the cracking of brittle matrix composites: Application to reinforced concrete. *Engineering Fracture Mechanics*, 213:182–196, 2019.